Machining Science and Technology, 15:21–46

ISSN: 1091-0344 print/1532-2483 online
DOI: 10.1080/10910344.2011.557950

Taylor & Francis
Taylor & Francis Group

3D FINITE ELEMENT MODELLING OF CHIP FORMATION PROCESS FOR MACHINING INCONEL 718: COMPARISON OF FE SOFTWARE PREDICTIONS

T. Ozel[1], I. Llanos[2], J. Soriano[2], and P.-J. Arrazola[2]
[1]*Manufacturing Automation Laboratory, Department of Industrial and Systems Engineering, Rutgers University, Piscataway, New Jersey, USA*
[2]*Faculty of Engineering, Mondragon University, Spain*

□ *Many efforts have been focused on the development of Finite Element (FE) machining models due to growing interest in solving practical machining problems in a computational environment in industry. Most of the current models are developed under 2D orthogonal plane strain assumptions, or make use of either arbitrary damage criterion or remeshing techniques for obtaining the chip. A complete understanding of the material removal process together with its effects on the machined parts and wear behaviour of the cutting tools requires accurate 3D computational models to analyze the entire physical phenomenon in materials undergoing large elastic-plastic deformations and large temperature changes as well as high strain rates. This work presents a comparison of 3D machining models developed using commercially available FE softwares ABAQUS/Explicit© and DEFORM™ 3D Machining. The work material is chosen as Inconel 718, a difficult-to-cut nickel-based alloy material. Computational results of temperature, strain and stress distributions obtained from the FE models for the effect of cutting speed are presented in comparison with results obtained from experimental tests. In addition, modified material model for Inconel 718 with flow softening is compared with the Johnson-Cook model. The predictions of forces and chip formation are improved with the modified material model.*

Keywords 3D computational modeling of machining, finite element simulations, machining of nickel-based alloys

INTRODUCTION

It is a fact that machining processes are still the most popular manufacturing technique in shaping and finishing metal parts due to their unmatched capability; thus, they are of great interest to industry. Despite their known advantages, selection of machining process parameters is often carried out with trial and error type approaches, thereby increasing cost

Address correspondence to P.-J. Arrazola, Faculty of Engineering, Mondragon University, Mondragón, 20500, Spain. E-mail: pjarrazola@eps.mondragon.edu

and process development lead time. To address this shortcoming, finite element (FE) modeling-based software tools have been developed and offered to simulate and predict the performance of a particular machining operation and minimize its experimental trials. However, there is great deal of uncertainty about the simulation approaches and the validity of their predictions especially from industrial end users. This paper focuses on three-dimensional (3D) modeling of the chip formation process in a face-turning operation using two different FE software and simulation approaches.

Since the early twentieth century, many researchers have been working to understand the chip formation process in cutting operations using analytical models pioneered by Merchant (1945), Lee and Shaffer (1951), Zorev (1966) and Oxley (1962). Initially, analytical models were limited to determining average values of basic process variables, such as shear and friction angles and cutting forces. In addition to those shear plane based solutions, analytical solutions were later developed to predict average temperatures, led by Trigger and Chao (1951), Loewen and Shaw (1964), Boothroyd (1963) and Tay et al. (1976) and more recently physics-based analytical solutions were introduced, led by Komanduri and Hou (2001), Molinari and Moufky (2005) and Karpat and Özel (2006) to predict detailed distributions of tool and work temperatures.

With the use of better material behavior models and elasto-visco-plastic deformations combined with the Finite Element Method (FEM), computational software has become available to obtain solutions for a rich set of field variables, providing much detailed insight for the chip formation processes. However, FEM based models have suffered from the difficulty of creating a chip that separates from the workpiece and depend upon artificial chip separation methods.

Most notably, updated Lagrangian FE formulations with remeshing have been offered by Sekhon and Chenot (1992) and Marusich and Ortiz (1995) to simulate material plastic flow around the tool tip for continuous and segmented chip formation. These approaches lead the development of these techniques, avoiding the use of an artificial material separation criterion and simplifying the mechanism of material separation (chip formation).

During the last decade, a major development in 3D FE models for machining has occurred with the advances in computers and numerical methods. Some of these models are based on the chip formation using damage criteria (Guo and Liu, 2002; Soo et al., 2004) for material separation or automatic techniques for remeshing of the workpiece (Ceretti et al., 2000; Özel, 2009).

In the meantime, other models have been created that use the Arbitrary Lagrangian Eulerian (ALE) formulation for chip formation in both 2D plane strain orthogonal cutting (Arrazola et al., 2003; Madhavan and

Adibi-Sedeh, 2005; Özel and Zeren, 2007; Haglung et al. 2008; Nasr et al. 2008) and 3D oblique cutting (Arrazola et al., 2006; Pantale et al., 1998; Arrazola et al., 2007; Arrazola and Özel, 2008; Llanos et al., 2009) thereby advancing the state-of-the-art towards more realistic FE models for practical industrial machining operations.

Because most of these industrial machining operations can be defined as 3D operations, the spatial calculation of field variables such as strain, stress and temperature should be provided in order to predict realistic fields for residual stresses on the machined workpiece or possible wear and damage zones on the cutting tool. There is both a growing inquisitiveness and ambiguity among industrial users about the effectiveness of FE-based machining simulations for predicting the accurate material deformation characteristics and machining performance.

In the present work, a comparison between machining models is carried out using two different FE modeling software packages. The purpose of such comparison is to provide a candid demonstration about the capabilities and predictions obtained using the commercially available FE modeling software.

The software employed in the FE simulations in this study are: i) general purpose FE code ABAQUS/Explicit© for 3D ALE formulation, and ii) DEFORM-3D Machining for 3D Updated Lagrangian formulation. The latter of these FE software packages is specifically focused on metal machining modeling. All the machining models have been tested under the same cutting condition, except that the cutting speed is varied.

Due to the uncertainty about input parameters and relevant differences between the two models about material modelling laws, friction modeling and FE formulations, the paper mainly focuses on a qualitative comparison of the predicted simulation results with experiments.

Nickel-based alloys are utilized in the hot sections of aircraft jet engines and gas turbines in aerospace and power industries since these alloys exhibit high strength at elevated temperatures, resistance to wear and chemical degradation. Machining of nickel based alloys, such as Inconel 718 (IN718), is considered extremely difficult, as widely reported in literature (Rahman et al. 1997; Sharman et al., 2004; Arunachalam et al., 2004a, 2004b; Ezugwu, 2005; Pawade et al., 2008). Low machinability of IN718 is due to its poor thermal conductivity, high toughness and work hardening behavior, and chemical affinity for the most tool materials (Rahman et al., 1997, Sharman et al., 2004; Ezugwu, 2005).

Many studies have been reported in machining of IN718 using carbide, coated carbide (Arunachalam et al., 2004a), cBN and ceramic (Arunachalam et al., 2004b) cutting tool materials. All of these studies

explored the tool life and sophisticated tool wear mechanisms when using these tool materials. The common agreement is that carbide tools show highest resistance to crater wear but the achievable surface cutting speeds are lower (<100 m/min). Pusavec et al. (2008) analyzed the performance of dry, MQL and cryogenic machining with uncoated carbide inserts.

Coated carbide tools improve the tool life and control some of the wear mechanisms (such as build up formation and abrasive wear) and provide some improvement in surface cutting speed (Arunachalam et al., 2004b; Pawade et al. 2008; Ranganath et al. 2009) but sudden failure of coating after a short cutting time followed by coating delamination is identified as the major problem. Ceramic tools achieved much higher cutting speeds (up to 300 m/min) but sudden notch wear and shorter tool life are seen as limitations. In addition, increasing micro hardness and depth of plastic deformation are reported when machining IN718 at higher cutting speeds (>100 m/min).

Hence, ceramics and cBN tools are not recommended for finish machining of nickel based alloys because of their poor performance due to excessive wear rates as a result of the high chemical reactivity of nickel based alloys with ceramics (Arunachalam et al., 2004a, Ezugwu 2005). In finishing operations for nickel based alloyed mission critical aerospace engine components in industry, uncoated carbide (WC/Co) tools at relatively low cutting speeds (30 m/min–60 m/min) are used due to concerns about the surface integrity produced (Sharma et al., 2004; Arunachalam et al., 2004a).

Compressive residual stresses are obtained at lower cutting speeds with uncoated carbide tools, and residual stresses tend to become tensile when machining with coated and ceramic tools at higher cutting speeds (Arunachalam et al., 2004a; 2004b). Therefore, analysis of machinability and surface integrity of nickel based alloys using FE software packages is of great interest to industry (Ranganath et al. 2009). In parallel, FE simulations to predict surface integrity have been also studied by several researchers (Outeiro et al., 2008, Ranganath et al. 2009, Özel 2009) to address the problem in machining produced surface integrity during finishing operations.

In this work, face turning of Inconel 718 nickel-based alloy (IN718) disk by using an uncoated carbide round insert was selected as the machining operation. First, a brief description of the FE models employed for 3D chip formation process will be given. Next, experimental set-up that was developed to measure the tool forces during machining will be described. Then, results obtained from FE simulations and experiments will be compared. Finally, an analysis of the results and overall conclusions will be reported.

3D FINITE ELEMENT MODELS FOR MACHINING

In this section, a brief description of the FE models employed using commercially available FE software is given. The input parameters to the FE models include constitutive model parameters representing the dynamic behavior of the work material, physical, thermal and mechanical properties of the work and tool materials, and contact conditions, such as friction and heat transfer coefficients. However, the most important of these is the constitutive material model parameters representing work material behavior under high strain, strain rate, and temperatures.

Constitutive Material Modeling for IN718

Dynamic material behavior data for Inconel 718 do not appear in the published literature with very few exceptions. Zhang et al. (1997) investigated strain-rate sensitivity of IN718 at high temperatures, a typical hot forming regime for turbine disk forging process, and presented compression test results at temperatures from 960 to 1040°C, with strain rates from 0.001 to $1.0\,s^{-1}$. One of the revealing results of that study was the flow softening behavior of the flow stress curve at strain rate of $1.0\,s^{-1}$ and temperature of 980°C above the strain value of 0.3. Since there was no flow stress data presented below 960°C, it was not possible to discuss possible dynamic strain aging behavior of IN718.

One of the few studies for dynamic material behavior for Ni-based super alloys is presented by Tancret et al. (2003), in which yield stress behavior with increasing temperature is given. In their work, dynamic strain aging phenomenon can be observed, where a sudden increase in stress around 600°C followed by sharp decrease with increasing temperatures is revealed. It was also reported that temperature dependent flow softening phenomenon occurs after a critical strain at high strains. It was claimed that flow softening with increasing strain at high strain rates but low temperatures is a result of athermal micro-mechanical phenomenon, such as rearranging dislocations, and at high temperatures thermally activated micro-mechanical phenomenon, such as increasing number of slip planes with phase change and dynamic recrystallization, etc.

Despite the other limitations reported by Warnecke and Oh [26] the thermo-visco plastic behaviour of the workpiece can be modeled by the Johnson-Cook constitutive equation [27], as given in Equation (1).

$$\bar{\sigma} = [A + B(\bar{\varepsilon})^n]\left[1 + C\ln\left(\frac{\dot{\bar{\varepsilon}}}{\dot{\bar{\varepsilon}}_0}\right)\right]\left[1 - \left(\frac{T - T_{room}}{T_{melt} - T_{room}}\right)^m\right] \tag{1}$$

In this equation, the constant A is the yield strength of the material at room temperature, $\bar{\varepsilon}$ is the equivalent plastic strain, and $\dot{\bar{\varepsilon}}$ is the normalized strain rate with a reference strain rate $\dot{\bar{\varepsilon}}_0$. In general, the constants A, B, C, and exponents n and m of the model are fitted to the data obtained by several material tests conducted at various strains, strain rates and temperatures.

However, to represent flow softening behavior of IN718, the Johnson-Cook material model in Equation (1) requires some modifications. Zhang et al. (2004) studied dynamic behavior of IN718 during superplastic (high strain) deformations and proposed a hyperbolic sine function to capture flow softening at increasing strains while retaining strain hardening at lower strains. They claimed that grain growth plays an important role in hardening and dynamic recovery, grain refinement and dynamic precipitation contribute to flow softening.

Later, DeMange et al. (2000) have studied effect of heat treatment on the room temperature quasi-static and high strain rate compression behavior of IN718 under annealed and aged conditions. Testing strain rate range for annealed material was 1796–3506 s^{-1}, while it was 1681–4581 s^{-1} for aged material. Strain hardening behavior of the material was significantly greater at annealed condition. Flow stress curves of the annealed material exhibited strong strain hardening at all strains, but the curves of the aged material showed sharp softening effect around a strain value of 0.1 and remained constant after strain value of 0.25. Pereiera and Lerch (2001) referred to that data and suggested the Johnson-Cook constitutive model without considering thermal softening effects as shown in Table 1. The Johnson-Cook material model parameters later developed for IN718 did not show any strain softening effect at elevated strain-rates and temperatures.

Sievert et al. (2003) utilized the Johnson-Cook constitutive model to simulate high speed machining of IN718. In their study, the J-C parameters for IN718 nickel alloy ($A = 450$ MPa, $B = 1798$ MPa, $C = 0.0134$, $n = 0.6522$, $m = 1.3$) were referred to Olschewski et al. (2001). In their work, they have also provided a ductile damage model. However, it is interesting to note

TABLE 1 The J-C Constitutive Model Parameters for IN718

Reference	A [MPa]	B [MPa]	C [-]	n [-]	m [-]	$\dot{\varepsilon}_0$ [s^{-1}]	Heat treat.
Pereira and Lerch (2001)	450	1798	0.0312	0.9143	0	1.0	annealed
Pereira and Lerch (2001)	1350	1139	0.0134	0.6522	0	1.0	aged
Uhlmann et al. (2007) Sievert et al. (2003) Olschewski et al. (2001)	450	1700	0.017	0.65	1.3	0.001	annealed
Mitrofanov et al. (2005)	1241	622	0.0134	0.6522	0	1.0	aged
Lorentzon et al. (2009)	1241	622	0.0134	0.6522	1.3	1.0	Aged

that these parameters are very close to those suggested by Pereira and Lerch (2001), and they are a combination of annealed (A and B) and aged (C and n) material conditions. At the time this article was prepared, the original source of these parameters and their underlying dynamic testing conditions were not known.

Mitrofanov et al. (2003, 2004, 2005) have studied FE simulation of machining IN718 nickel alloy under ultrasonic assisted turning conditions in a series of publications with few distinctions, most appeared in various journals, and used Ramberg-Osgood constitutive equation in their earlier work (Mitrofanov et al., 2003) and then the J-C material model as suggested by Pereira and Lerch (Pereira and Lerch, 2001) in a later work (Mitrofanov et al., 2005).

In their later work, Mitrofanov et al. (2005) suggested new set of the J-C model parameters for IN718, namely $A = 1241$ MPa, $B = 622$ MPa, $C = 0.0134$, $n = 0.6522$. Where parameters A and B were calculated from quasi-static material property data and rate sensitivity, C, and strain hardening, n, parameters were adopted from Pereira and Lerch (2001). Unfortunately, they failed to disclose the details of these calculations and validity of the new parameters against the dynamic testing data. In addition, they claimed that flow stress softening with increasing temperatures for IN718 nickel alloy is less than 5% on the flow stress and incorrectly assumed thermal softening is negligible (i.e., $m = 0$).

Uhlmann et al. (2007) also utilized the Johnson-Cook material model to simulate cutting of IN718 and used model parameters proposed by Sievert et al. (2003) and Olschewski et al. (2001). They have compared simulation results from ABAQUS-2D, ABAQUS-3D and DEFORM-2D, where a ductile damage model for material separation was implemented in ABAQUS. Lorentzon et al. (2009) used model parameters A, B, C, n from Mitrofanov et al. (2005) and $m = 1.3$ from Sievert et al. (2003) and Olschewski et al. (2001). Melting temperature for IN718 nickel based alloy is taken as $T_m = 1297\ ^\circ$C.

3D FE Modeling of Machining with ALE Formulation

In 3D FE modeling of machining with Arbitrary Lagrangian Eulerian (ALE) formulation, ABAQUS/Explicit, general purpose FE software, is employed. A 3D single point turning model similar to the models proposed by Arrazola et al. (2006) and Arrazola and Özel (2008) has been developed here. Thermo-mechanically coupled FE simulations have been performed. Figure 1 shows a schematic view of the model, as well as the shape and mesh employed for the cutting tool and the machined material.

An ALE formulation has been employed in the model by allowing material entry flow to the workpiece from *Entry_Material*, exit flow from

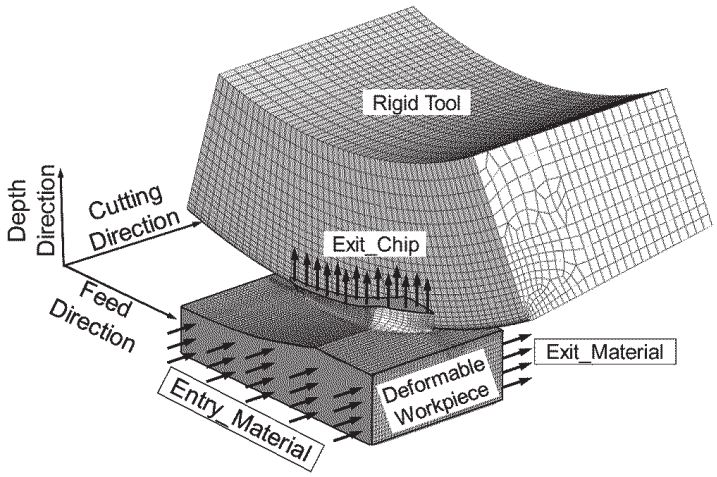

FIGURE 1 3D ALE FE model for chip formation process using ABAQUS/Explicit.

the workpiece with *Exit_Material* and from the chip with *Exit_Chip Eulerian* surfaces as shown in Figure 1. ALE numerical formulation allows the FE model to predict state variables without using any artificial criterion (physical or geometrical) to obtain the material separation of the chip from the workpiece.

The tool is considered as a rigid body while the workpiece is modeled as deformable (elastic-viscoplastic), due to the differences in their mechanical characteristics and the need for the process outputs. The Coulomb friction law has been selected for modeling contact friction along the tool-chip interface. The heat transfer from the chip into the tool body is allowed along the tool-chip contact area. In the workpiece mesh, C3D8RT elements are employed with eight node bricks with tri-linear displacement, temperature calculation, reduced integration and hourglass control. The element size in the workpiece mesh varies from 4 μm to 100 μm depending on the zone. The mass scaling was applied in some small elements close to the cutting edge, in order to reduce calculation time.

Nevertheless, it should be noted that in ABAQUS ALE formulation only the mechanical solution is affected by the mass scaling and not the thermal one. Therefore, mass scaling does not affect temperature predictions but it may affect the accuracy of the mechanical load related field variables. To verify this, the authors analyzed the influence of mass scaling in oblique machining operations in ABAQUS with ALE formulation models. In that work, Llanos et al. (2009) concluded that the simplifications for lowering the calculation time with mass scaling had small and easily detectable effects on the results from the numerical model ((less than 4% in the case of the cutting forces and less than 1% in the case of temperature values).

TABLE 2 Input Parameters for the ABAQUS FE Model

Parameter		Value
Johnson-Cook model	A [MPa]	1241
	B [MPa]	622
	n [-]	0.6522
	C [-]	0.0134
	m [-]	1.3
Friction Coefficient	μ [-]	0.6

In Table 2, some of the input parameters for work material (IN718) and tool-work contact conditions that are used in the ABAQUS FE model are shown. The parameters of the Johnson-Cook constitutive model were obtained from the work by Lorentzon et al. (2009). Lorentzon et al. (2009) used the Coulomb friction model for the tool-chip interface contact conditions in FE simulations of IN718 nickel alloy. In their study, a mean friction coefficient of 1.0 was selected as calibrated from the simulated and measured forces for the cutting speed of $V = 45$ m/min and feed of $f = 0.1$ mm. In another study by Ahmed et al. (2006), a friction coefficient of 0.5 for the shear friction model was suggested for the cutting speed of $V = 8.1$ m/min, feed of $f = 0.1$ mm and depth of cut of $a_p = 0.4$ mm. In this study, a friction coefficient of 0.6 for the Coulomb friction model was selected for the cutting conditions of $V = 30$ and 70 m/min, feed of $f = 0.25$ mm and depth of cut of $a_p = 0.15$ mm.

To manage the computation time in the presented model, mass scaling option is used, which basically increases material density in a controlled manner, in order to reduce the computational time. It has been set up to lower time increment to the value of 10^{-8} s and to obtain a reduction of computational time from 170 hours to 10 hours for 1 milliseconds of machining time, in a 2.4 GHz computer with 2 GB RAM.

3D FE Modeling of Machining with Updated Lagrangian Formulation

In 3D FE modeling of machining with updated Lagrangian formulation, machining module of the DEFORM- 3D finite element software specialized for modeling of machining operations is used. The software allows a coupled modeling of deformation and heat transfer using implicit integration method. In this program, updated Lagrangian formulation combined with automatic remeshing techniques is employed to simulate visco-plastic material flow around the cutting tool tip for material separation. The model shown in Figure 2 has been created.

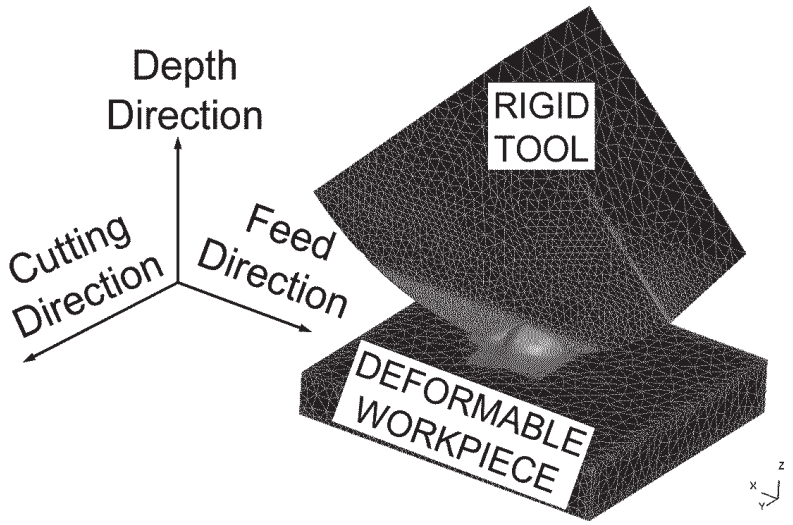

FIGURE 2 3D FE model for machining using DEFORM-3D.

At first, the material behavior of the workpiece is modeled by the Johnson-Cook constitutive material model as proposed by Lorentzon et al. (2009) similar to the ABAQUS FE model. The workpiece is modeled using 75000 elements as an elastic-viscoplastic body. The tool was modeled as tungsten carbide material with properties given in Table 4 and a rigid body represented with 85000 elements.

As discussed earlier here, modifications to the Johnson-Cook material model have been offered in order to represent temperature dependent flow softening at high strain in IN718 nickel based alloy. Localized temperature dependent flow softening phenomenon can be described as offering less resistance to plastic deformations due to rearrangement of dislocations caused by subsequent cycling in hard materials. This phenomenon is usually seen during an increase in strain beyond a critical strain value. Similar characteristics have also been reported for nickel alloys (Zhang et al., 2004; DeMange et al., 2009).

This may be due to increasing activity in microstructural changes at elevated strains, strain-rates and temperatures such as dynamic recrystallization or phase change or other thermal-mechanical deformation characteristics of Inconel718 nickel alloy (DeMange et al., 2009). Recently reported studies offered modified material models that include flow softening phenomenon at elevated strain and strain rates for titanium alloy Ti-6Al-4V by using a *tanh* function with additional parameters (Calamaz et al., 2008). Similar approach is taken in this work to include flow softening combined with strain hardening, strain-rate sensitivity and temperature softening of IN718 nickel alloy (Özel, 2009).

TABLE 3 Input Parameters for the DEFORM-3D FE Model

Parameter		Value
Modified Johnson-Cook Model	A [MPa]	1241
	B [MPa]	622
	n [-]	0.6522
	C [-]	0.0134
	m [-]	1.3
	D [-]	0.6
	S [-]	0.0
	s [-]	5.0
	r [-]	1.0
Friction coefficient	μ [-]	0.6

For the use in the DEFORM-3D simulations, the J-C constitutive material model is modified as given in Equation (2) to include the temperature-dependent flow softening effect in addition to strain and strain rate hardening and thermal softening.

$$\bar{\sigma} = [A + B(\bar{\varepsilon})^n]\left[1 + C\ln\left(\frac{\dot{\bar{\varepsilon}}}{\dot{\bar{\varepsilon}}_0}\right)\right]\left[1 - \left(\frac{T - T_0}{T_{melt} - T_0}\right)^m\right] \times \left[D + (1 - D)\left[\tanh\left(\frac{1}{(\varepsilon + S)^r}\right)\right]^s\right] \tag{2}$$

The modified J-C material parameters for IN718 are given in Table 3. The flow stress curves using the modified J-C material parameters are given in Figure 3. Similar to the flow stress curves reported by Zhang et al. (2004) and DeMange et al. (2009), flow softening begins after a stain value of 0.4 and strain hardening resumes after the strain value of 1.2. These flow stress curves have been implemented in the DEFORM-3D finite element model for IN718 nickel based alloy.

In DEFORM-3D FE model, frictional contact along the tool/chip interface can be modeled by the shear friction law as well as Coulomb friction low. Shear friction law, which is defined as $m = \tau/k$ where τ is frictional shear stress and k is the work material shear flow stress, is commonly used at the severe contact conditions existing in metal forming and metal cutting problems (Özel, 2009). Although both Coulomb friction and shear friction can be implemented in DEFORM-3D FE software, Coulomb friction along the chip-tool interface is implemented to be able to compare the simulation results obtained under same friction conditions. Therefore, a mean (average) friction coefficient of $\mu = 0.6$ was used for the uncoated carbide (WC/Co) cutting tool in machining of the nickel based alloy IN718 in this study.

Four-node tetrahedral finite elements with minimum element size of 7 μm, a maximum element size of 210 μm and a size ratio of 30 are used.

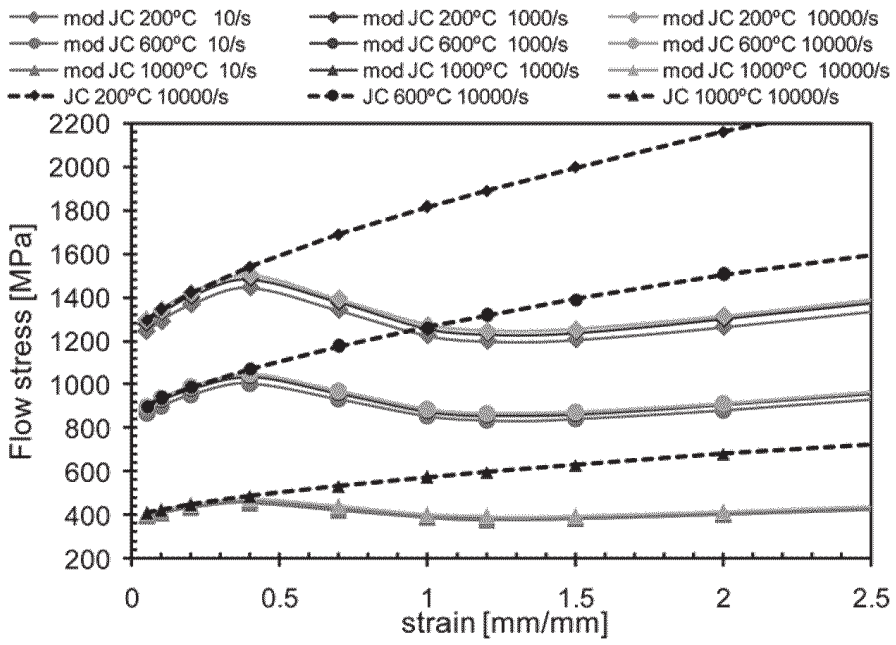

FIGURE 3 Flow stress curves of the modified material model for IN718 (Özel, 2009).

Very fine mesh in the vicinity of the tool and workpiece contact is achieved in order to simulate chip formation accurately. The computation time for the models developed under DEFORM3D Machining software was about 28 hours to obtain a 1 millisecond machining time. The simulations were carried out in a 2 GHz computer with 2GB RAM memory.

EXPERIMENTAL SETUP

Face turning tests have been carried out on a precipitation-hardened IN718 workpiece, as shown in Figure 4a (disc obtained from a plate), by using ISO P10 grade cemented carbide (WC/Co) inserts, which were measured to meet the requirement of a cutting edge radius (r_β) of $40 \pm 5\,\mu m$.

A specially developed machining setup, as shown in Figure 4b, was utilized to obtain experimental data of cutting forces for the qualitative validation of the numerical results. A piezoelectric turret type dynamometer (Kistler 9121) was used for the measurement of cutting forces during the machining tests in the cutting (F_c), feed (F_f), and thrust (F_p) directions. The standard deviations of these forces were 15, 6, and 17 N, respectively, which were calculated from the forces obtained in four replications at the same experimental condition. In each experiment a fresh cutting tool is used.

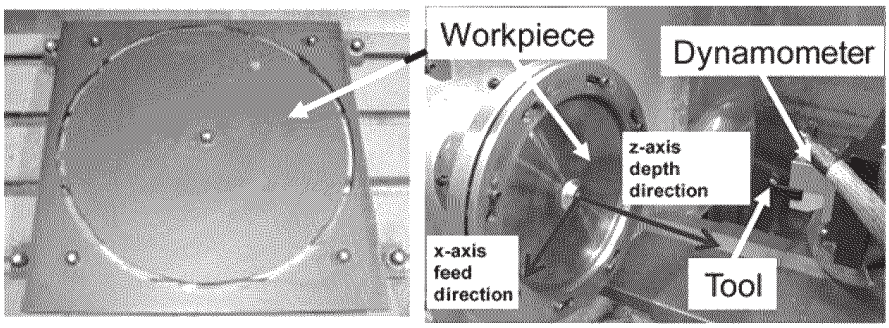

FIGURE 4 (a) Shape of the workpiece (disc obtained form a plate) obtained from a rectangular plate. (b) Experimental set-up for cutting force measurement.

Because no lubricant has been used during the cutting tests, severe tool wear has been observed on the cutting tool. Thus, the measurement of the forces has been realized before the tool wear would increase.

RESULTS FROM FINITE ELEMENT SIMULATIONS

The detailed tool geometry, cutting conditions and tool material properties employed in experimental tests and numerical simulations are given in Table 4. FE models developed as discussed previously will be evaluated by using a comparison of the results obtained under two different cutting speeds (30 m/min and 70 m/min) against experimental results.

TABLE 4 Tool geometry, Process Parameters and Tool Material Properties Used in the FE Models

Parameter	Value
Tool geometry	
Tool nose radius (R) [mm]	4
Tool edge radius (r_β) [μm]	40
Back rake angle (γ) [°]	0
Side rake angle (i) [°]	0
Clearance angle (α) [°]	7
Process	
Cutting speed (V) [$m \cdot min^{-1}$]	30 and 70
Feed (f) [$mm \cdot rev^{-1}$]	0.25
Depth of cut (a_p) [mm]	0.15
Tool material (WC/Co)	
Density (ρ) [$kg \cdot m^{-3}$]	15000
Poisson ratio (ν) [-]	0.2
Elasticity (E) [$N \cdot m^{-2}$]	800
Thermal conductivity (λ) [$W \cdot m^{-1}\,°C^{-1}$]	46
Specific heat (c) [$J \cdot Kg^{-1} \cdot K^{-1}$]	203
Thermal expansion (α) [$mm \cdot mm^{-1} °C^{-1}$]	4.7×10^{-6}

TABLE 5 Comparison of the Measured and Predicted Forces with Percentage Prediction Error

Test	Cutting forces		
	F_c [N]	F_f [N]	F_p [N]
EXPERIMENTAL ($V=30$ m/min)	175	37	180
EXPERIMENTAL ($V=70$ m/min)	173	30	182
ABAQUS ($V=30$ m/min) with J-C model	306 (75%)	29 (22%)	204 (13%)
ABAQUS ($V=70$ m/min) with J-C model	274 (58%)	24 (20%)	189 (4%)
DEFORM ($V=30$ m/min) with J-C model	349 (99%)	34 (8%)	249 (38%)
DEFORM ($V=70$ m/min) with J-C model	304 (76%)	27 (1%)	200 (10%)
DEFORM ($V=30$ m/min) with modified J-C model	222 (27%)	23 (38%)	173 (4%)
DEFORM ($V=70$ m/min) with modified J-C model	188 (9%)	21 (30%)	157 (14%)

In FE simulations, the resultant field variables have been extracted after 1 millisecond (ms) of cutting time. This short cutting time is assumed sufficient for the field variables to reach a steady-state.

Measured mean forces from experimental tests and predicted forces from numerical simulations are shown in Table 5. A graphical comparison of these forces is given in Figure 5. Indicators are also placed to show the variations in measured forces. As can be seen in this figure, the cutting forces predicted using updated Lagrangian formulation with DEFORM software and the modified Johnson-Cook material model provide a better match (about 3% error) whereas predicted thrust (passive) forces show higher error (about 20%). Predicted cutting forces using the Johnson-Cook material model with updated Lagrangian formulation (DEFORM) and ALE formulation (ABAQUS) show much greater mismatch (75% error) with the experimentally measured ones.

In addition, a comparison of predicted force with time obtained from FE simulations with updated Lagrangian formulation using the modified Johnson-Cook material model with the measured mean forces are given in Figure 6. The transient forces during chip formation can be observed from these figures. Since a larger section of the work material is removed using 70 m/min cutting speed for 1.2 ms of cutting time, the force vs. time plot shown in Figure 6b indicates a more intense cyclical force behavior.

In the case of the ABAQUS FE simulations, the predicted cutting forces were found much higher than the thrust forces. Interestingly, forces obtained from ABAQUS at higher cutting speed ($V=70$ m/min), as shown in Figure 7, were lower after a cutting time of 0.4 milliseconds as a result of increasing cutting temperatures and corresponding decrease in the flow stress.

The detailed FE simulation results about process variables (temperature, strain and stress) corresponding to the state of the machined work material, chip and tool have been extracted for the comparison of both models. These results can be seen in Table 6. Since there is no

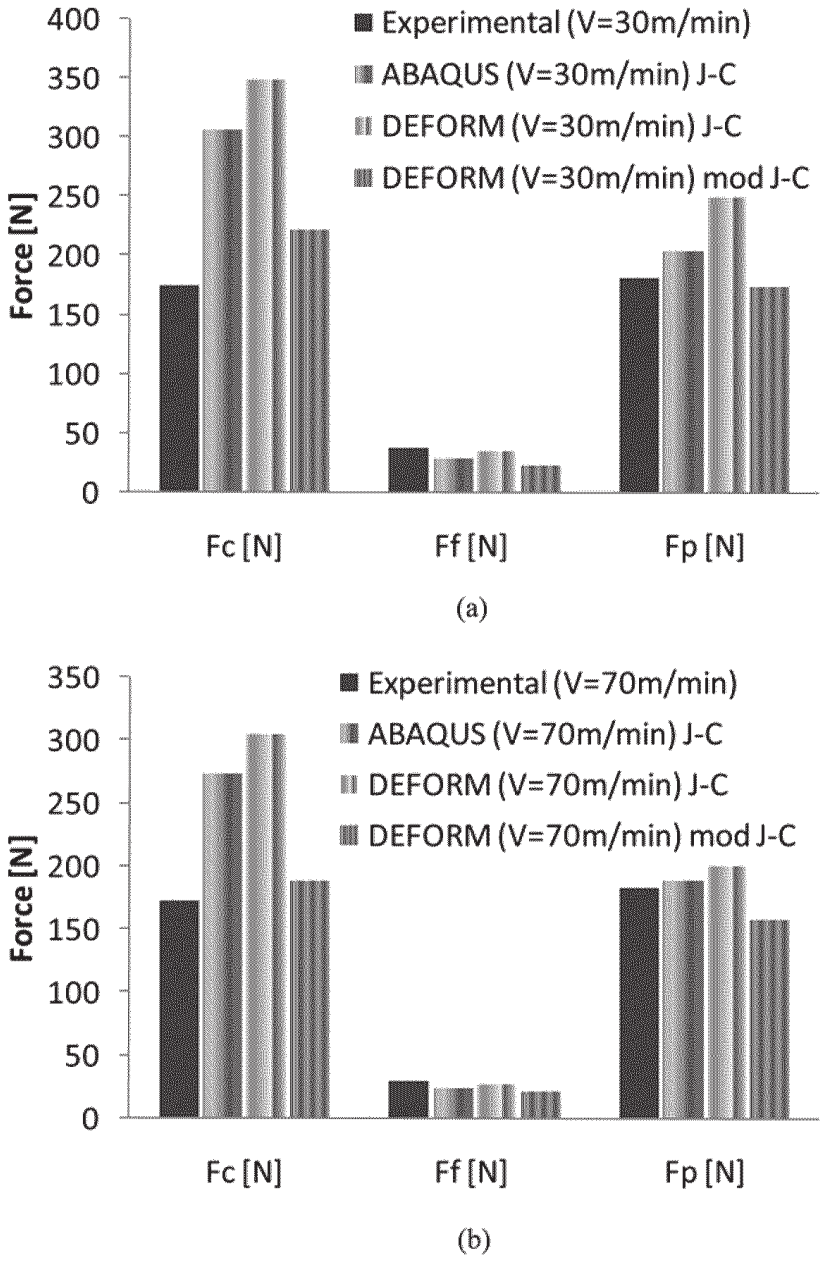

FIGURE 5 Comparison of the predicted and experimentally measured machining forces.

experimental measurement for these variables, it is difficult to make a judgment about the accuracy of the predictions. Hence, a qualitative comparison is provided. Predicted temperatures were seen higher in ABAQUS model compared to DEFORM model. However, both models are in agreement that the increased cutting speed raises the predicted temperatures in workpiece, chip and the tool.

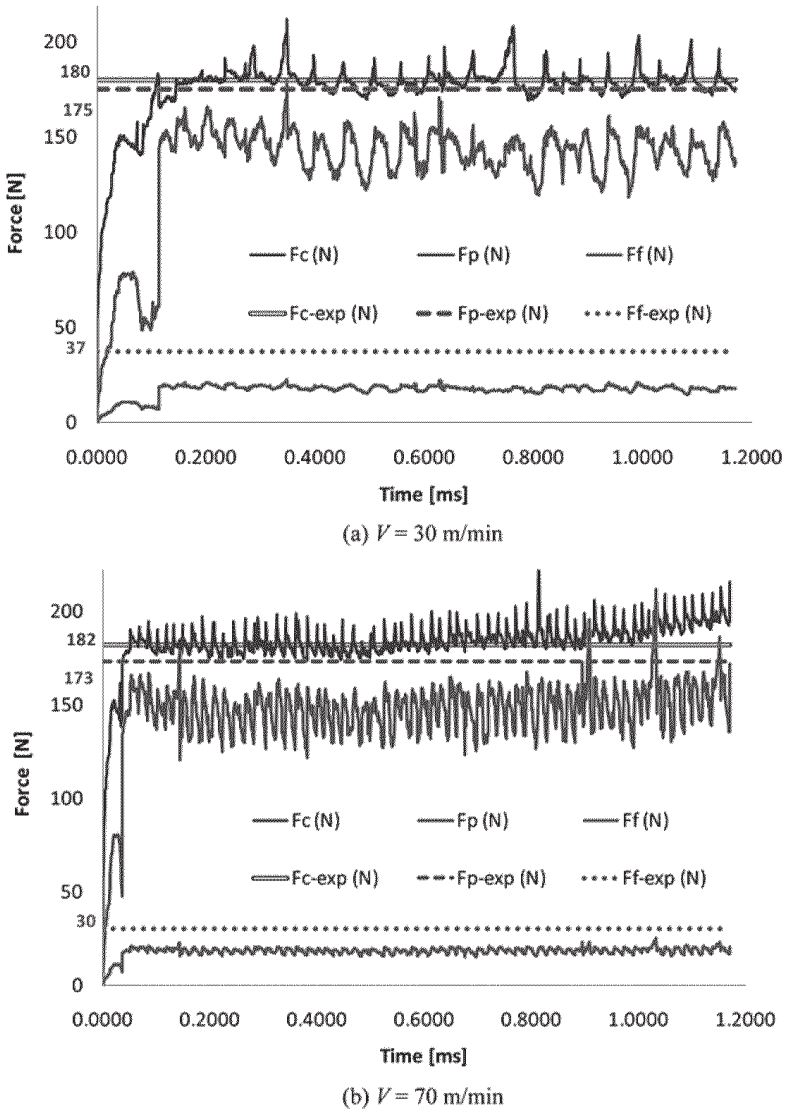

FIGURE 6 Comparison of the predicted force vs. time (DEFORM-3D with the modified J-C model) and measured mean forces (F_c, F_p, F_f).

In addition, as can be observed from Figures 8 and 9, the advantage of predicting incipient to steady-state chip formation using updated Lagrangian formulation, as in DEFORM-3D software, is that the chip curl and some serration can be investigated. In Figures 8b and 9b, the chip length is greater than the chip length at lower cutting speed, since both images are taken at the cutting time of 1 ms. There is also high heat concentration at the root of the chip and around the tool edge radius location, as shown in Figures 8 and 9 (DEFORM3D model) and Figure 10 (ABAQUS model).

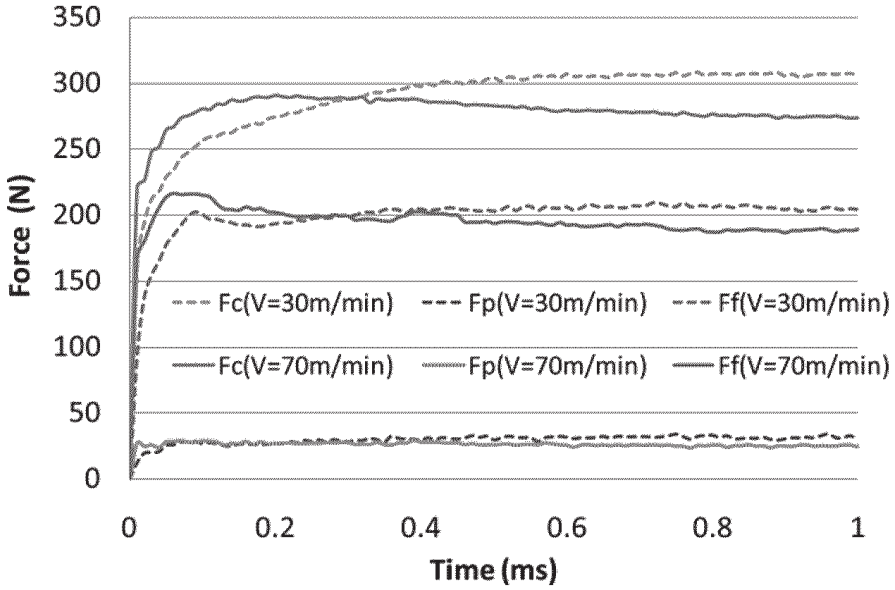

FIGURE 7 Evolution of the predicted forces with time (ABAQUS/Explicit).

The low thermal conductivity of the IN718 is responsible for this high heat concentration at the tool tip. This heat localization is also reflected upon the tool tip, as indicated in Figures 11 and 12, as obtained from DEFORM-3D, and in Figure 13, as obtained from ABAQUS/Explicit. Obviously, increasing heat generation is more pronounced at the higher cutting speed condition ($V = 70$ m/min), as shown in Figures 11b and 12b (DEFORM-3D model) and Figure 13b (ABAQUS model).

TABLE 6 Comparison of the Results Obtained Using ABAQUS and DEFORM FE Models

	Tool	Workpiece				Chip		
Test	*Temp* [K]	*Temp* [K]	ε_{eff} [-]	$\dot{\varepsilon}_{eff}10^3$ [s^{-1}]	σ_{VM} [GPa]	*Temp* [K]	ε_{eff} [-]	σ_{VM} [GPa]
ABAQUS ($V = 30$ m/min) the J-C model	934	968	4.29	20.3	2.14	959	4.19	2.24
ABAQUS ($V = 70$ m/min) the J-C model	1131	1104	4.56	36.8	2.06	1136	5	2.28
DEFORM ($V = 30$ m/min) the J-C model	953	993	6.02	13.6	3.00	873	4.01	2.07
DEFORM ($V = 70$ m/min) the J-C model	1206	1190	5.81	33.0	1.68	1178	4.81	2.30
DEFORM ($V = 30$ m/min) the modified J-C model	825	817	3.9	13.2	1.4	780	3.7	1.50
DEFORM ($V = 70$ m/min) the modified JC model	1006	1003	3.4	32.5	1.90	903	3.9	1.75

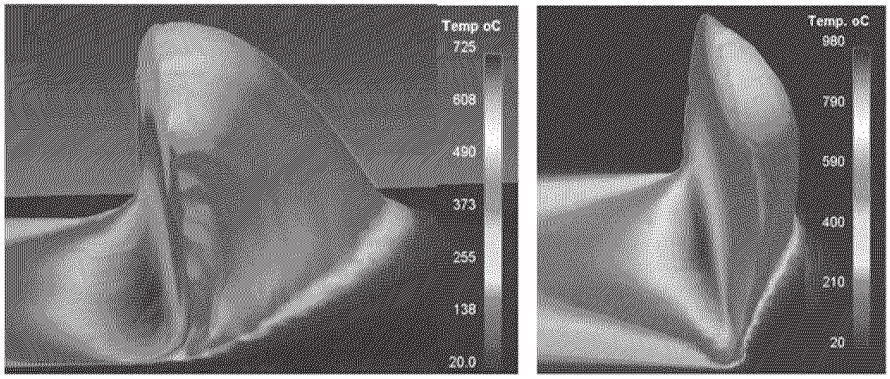

(a) $V = 30$ m/min (b) $V = 70$ m/min

FIGURE 8 Temperature distributions in the chip and the workpiece after 1 ms of cutting time (DEFORM-3D using the J-C model).

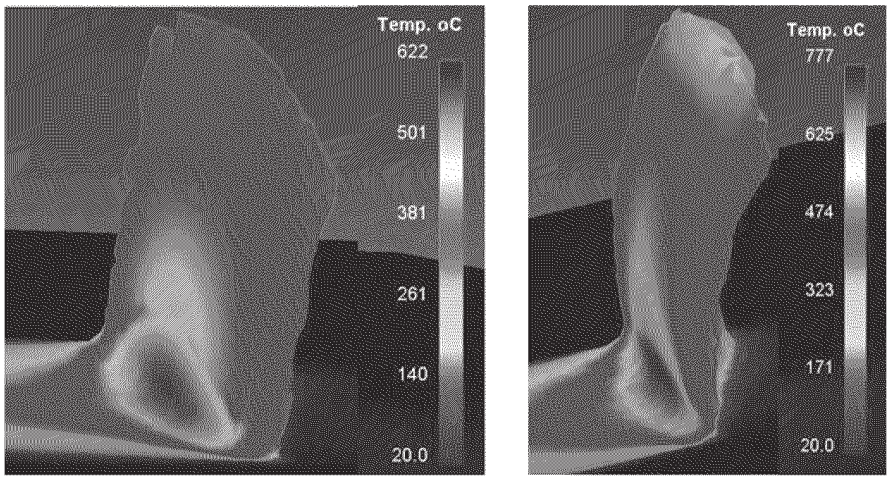

(a) $V = 30$ m/min (b) $V = 70$ m/min

FIGURE 9 Temperature distributions in the chip and the workpiece after 1 ms of cutting time (DEFORM-3D using the modified J-C model).

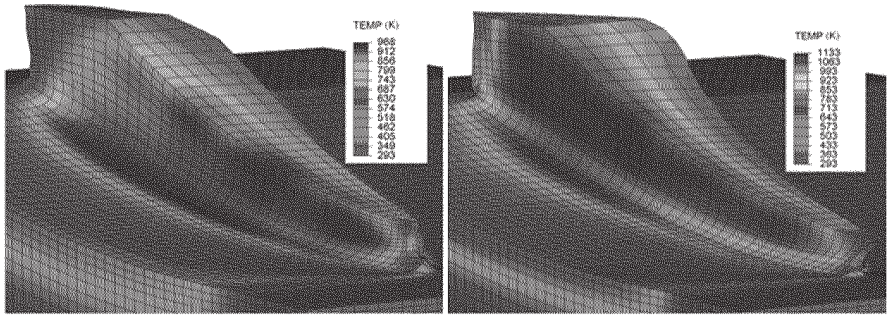

(a) $V = 30$ m/min (b) $V = 70$ m/min

FIGURE 10 Temperature distributions in the chip and the workpiece after 1 ms of cutting time (ABAQUS).

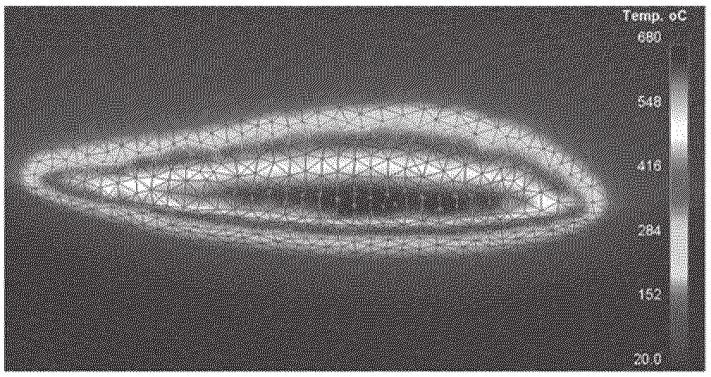

(a) $V = 30$ m/min

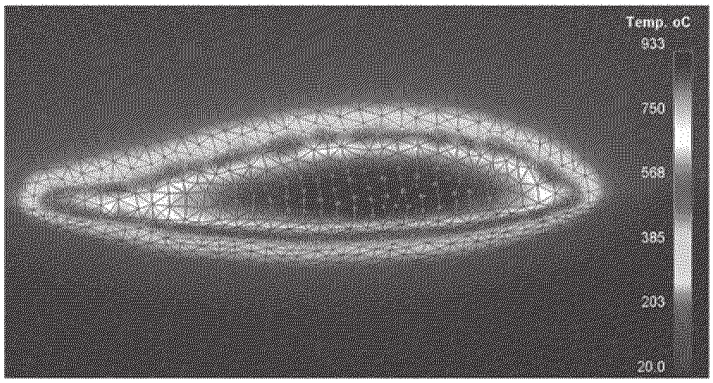

(b) $V = 70$ m/min

FIGURE 11 Temperature distributions in the tool after 1 ms of cutting time (DEFORM-3D using the J-C model).

Effective strain distributions are also obtained from the FE simulations, as shown in Figures 14, 15 and 16 using DEFORM-3D and ABAQUS models, respectively. As can be seen from these figures, overall, these predictions are in close agreement with each other.

Effective stress and von Mises stress distributions are also obtained from the FE simulations as shown in Figures 17, 18 and 19 using DEFORM-3D with the J-C model, DEFORM-3D with the modified J-C model, and ABAQUS models respectively. The stress predictions obtained using DEFORM-3D with the modified J-C model and ABAQUS/Explicit are in close agreement with each other.

CONCLUSIONS

In this study, a comparison between 3D FE models and experimental results when machining Inconel 718 nickel-based alloy is presented. The FE models are developed as close as possible using ABAQUS and DEFORM 3D software packages and simulations are run at the same cutting

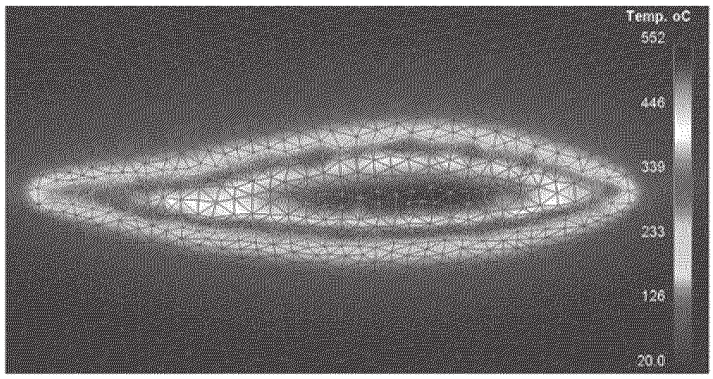

(a) $V = 30$ m/min

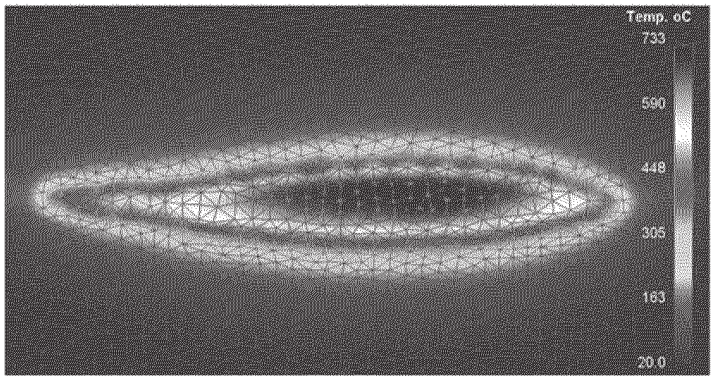

(b) $V = 70$ m/min

FIGURE 12 Temperature distributions in the tool after 1 ms of cutting time (DEFORM-3D using the modified J-C model).

conditions as the experimental tests, for two different cutting speeds. A modified Johnson-Cook material model for IN718 nickel alloy is also presented to account for the flow softening effect reported in literature. The effects of modified material model on predicted forces, and temperature, strain and stress fields are investigated. The following general observations are obtained:

- 3D FE models (both DEFORM-3D and ABAQUS/Explicit) for simulation of chip formation in machining processes are possible to investigate process variables and design cutting tools and optimize cutting conditions.
- Predicted forces by using the Johnson-Cook material model parameters reported by Mitrofanov, Sievert and Lorentzon showed a larger mismatch with experimental forces. However, the modified J-C material model for IN718 has given much closer force predictions.
- When comparing predicted cutting forces, best results were obtained using modified Johnson-Cook material model and Updated Lagrangian (DEFORM-3D) approach.

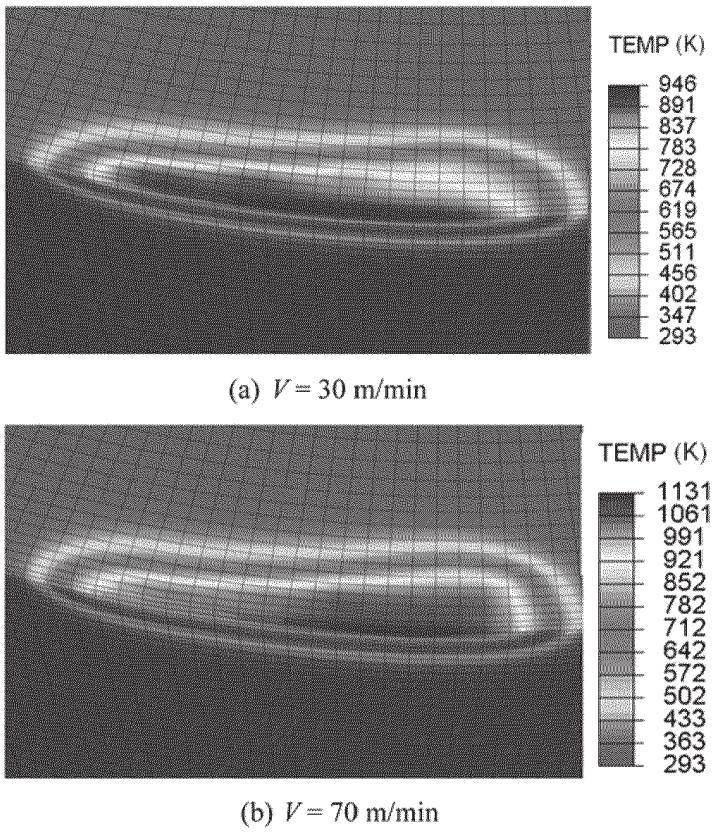

FIGURE 13 Temperature distributions in the tool after 1 ms of cutting time (ABAQUS).

- Predicted cutting forces were larger than experimental forces using the Johnson-Cook material model with both Updated Lagrangian (DEFORM-3D) and ALE (ABAQUS/Explicit) models.

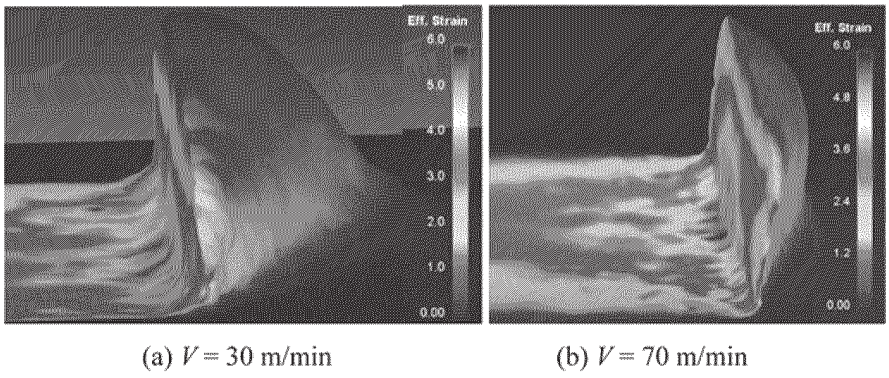

FIGURE 14 Effective strain distributions in the chip and the workpiece after 1 ms of cutting time (DEFORM-3D using the J-C model).

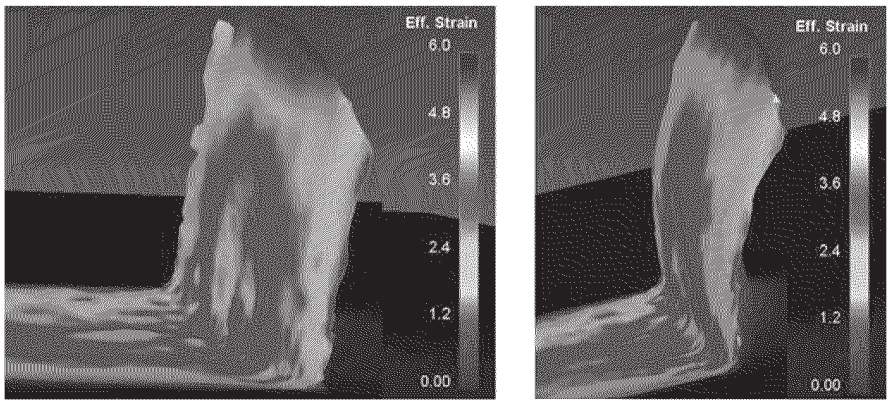

(a) $V = 30$ m/min (b) $V = 70$ m/min

FIGURE 15 Effective strain distributions in the chip and the workpiece after 1 ms of cutting time (DEFORM-3D using the modified J-C model).

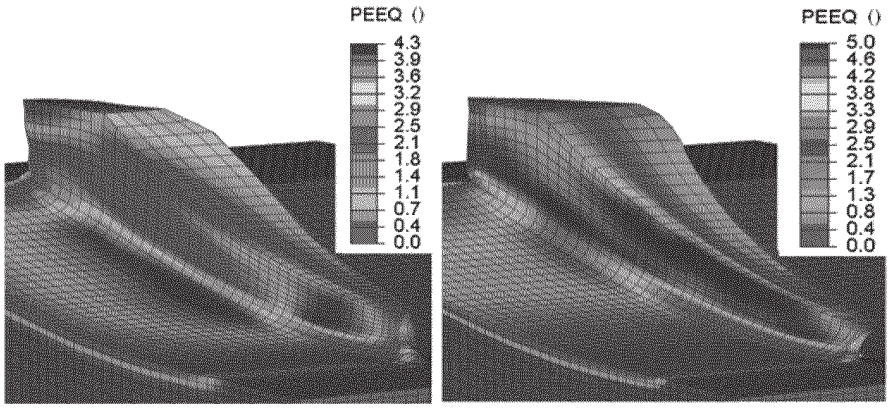

(a) $V = 30$ m/min (b) $V = 70$ m/min

FIGURE 16 Effective strain distributions in the chip and the workpiece after 1 ms of cutting time (ABAQUS).

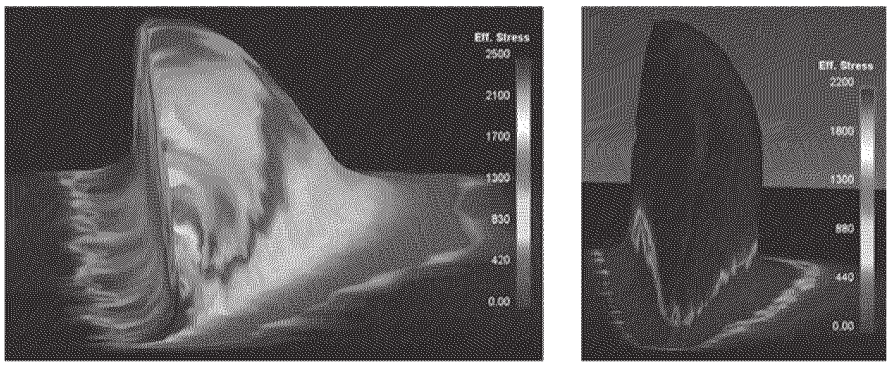

(a) $V = 30$ m/min (b) $V = 70$ m/min

FIGURE 17 Effective stress (von Mises) distributions (MPa) in the chip and the workpiece after 1 ms of cutting time (DEFORM-3D using the J-C model).

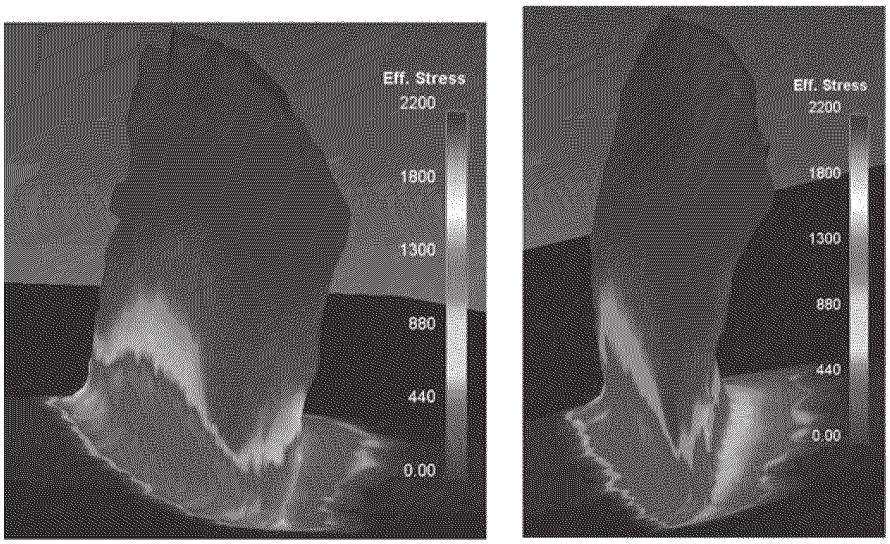

(a) V = 30 m/min (b) V = 70 m/min

FIGURE 18 Effective stress (von Mises) distributions (MPa) in the chip and the workpiece after 1 ms of cutting time (DEFORM-3D using the modified J-C model).

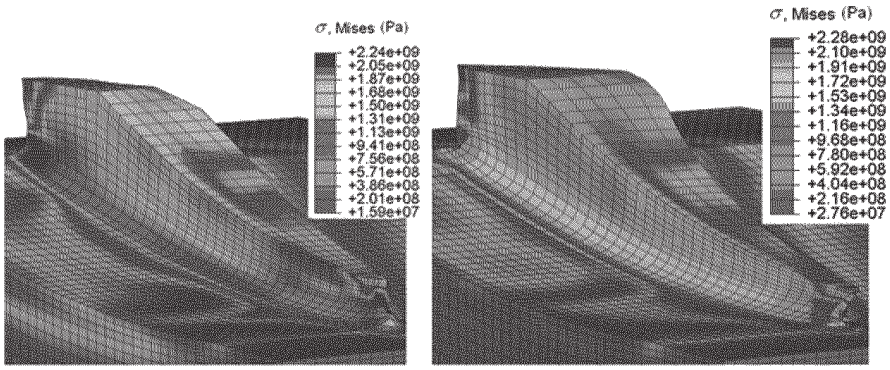

(a) V = 30 m/min (b) V = 70 m/min

FIGURE 19 Effective stress (von Mises) distributions in the chip and the workpiece after 1 ms of cutting time (ABAQUS).

- Predicted temperature values are found about the same as obtained from ABAQUS/Explicit and DEFORM-3D but lower when using modified Johnson-Cook model.
- Predicted strain and stress values are found similar in the results obtained from DEFORM-3D and ABAQUS/Explicit software.

REFERENCES

Ahmed, N.; Mitrofanov, A.V.; Babitsky, V.I.; Silberschmidt, V.V. (2006) Analysis of material response to ultrasonic vibration loading in turning Inconel 718. *Materials Science and Engineering A*, 424: 318–325.

Arrazola, P.J.; Pujana, J.; Llanos, I., Villar, A., Ugarte, D., Aguirre, A., Gallego, I., Le Maître F. (2006) Finite element modeling of oblique cutting. *Proceedings of the 9th CIRP International Workshop on Modelling Machining Operations*, pp. 101–112.

Arrazola, P.J.; Llanos, I.; Villar, J.A.; Ugarte, D.; Marya, S. (2007) 3D Finite Element Modelling of Chip Formation Process, In *Proceedings of the 10th CIRP International Workshop on Modeling of Machining Operations*, Regio-Calabria, Italia.

Arrazola, P.J.; Meslin, F.; Marya, S. (2003) Sensitivity study in numerical cutting modelling, In *Procedings of the 7th CIRP International Workshop on Modelling Machining Operations*, pp. 83–90.

Arrazola, P.J.; Özel, T. (2008) Numerical modelling of 3-D hard turning using Arbitrary Eulerian Lagrangian finite element method. *International Journal of Machining and Machinability of Materials*, 3(3): 238–249.

Arunachalam, R.M.; Mannan, M.A.; Spowage, A.C. (2004b) Residual stress and surface roughness when facing age hardened Inconel 718 with CBN and ceramic cutting tools. *International Journal of Machine Tools and Manufacture*, 44: 879–887.

Arunachalam, R.M. Mannan, M.A.; Spowage, A.C. (2004a) Surface integrity when machining age hardened Inconel 718 with coated carbide cutting tools. *International Journal of Machine Tools and Manufacture*, 44: 1481–1491.

Boothroyd, G. (1963) Temperatures in orthogonal metal cutting. *Proc. Inst. Mech. Eng.*, 177: 789–810.

Calamaz, M.; Coupard, D.; Girot, F. (2008) A new material model for 2D numerical simulation of serrated chip formation when machining titanium alloy Ti–6Al–4V. *International Journal of Machine Tools & Manufacture*, 48, 275–288.

Ceretti, E.; Lazzaroni, C.; Menegardo, L.; Altan, T. (2000) Turning simulations using a three-dimensional FEM code. *Journal of Materials Processing Technology*, 98: 99–103.

DeMange, J.J.; Pereira, J.M.; Lerch, B.A.; Prakash, V. (2000) Ballistic impact behavior of Ni-based super alloys with applications to engine fan blade containment. In *Proceedings of the SEM IX International Congress on Experimental Mechanics*, Orlando, FL, June 5–8, pp. 344–347.

DeMange, J.J.; Prakash, V.; Pereira, J.M. (2009) Effects of material microstructure on blunt projectile penetration of a nickel-based super alloy. *International Journal of Impact Engineering*, 36: 1027–1043.

Ezugwu, E.O. (2005) Key Improvements in the machining of difficult-to-cut aerospace superalloys. *International Journal of Machine Tools & Manufacture*, 45: 1353–1367.

Guo, Y.B.; Liu, C.R. (2002) 3D FEA modeling of hard turning. *ASME Journal of Manufacturing Science and Engineering*, 124: 189–199.

Haglund, A.; Kishawy, H.A.; Rogers, R.J. (2008) An exploration of friction models for the chip tool interface using an arbitrary Lagrangian-Eulerian finite element model. *Wear*, 265(3–4): 452–460.

Johnson, G.R.; Cook, W.H. (1983) A constitutive model and data for metals subjected to large strains, high strain rates and high temperatures. *Proceedings of 7th International Symposium on Ballistics*, pp. 541–547.

Karpat, Y.; Özel, T. (2006) Predictive analytical and thermal modeling of orthogonal cutting process. Part I: Predictions of tool forces, stresses and temperature distributions. *ASME Journal of Manufacturing Science and Engineering*, 128: 435–444.

Komanduri, R.; Hou, Z.B. (2001) Thermal modeling of the metal cutting process, Part 1: temperature rise distribution due to shear plane heat source. *International Journal of Mechanical Sciences*, 42: 1715–1752.

Lee, E.H.; Shaffer, B.W. (1951) The theory of plasticity applied to a problem of machining. *Transactions of the ASME, Journal of Applied Mechanics*, 18: 405–413.

Leowen, E.G.; Shaw, M.C. (1964) On the analysis of cutting tool temperatures. *Transactions of ASME*, 71: 217–231.

Llanos, I.; Villar, J.A.; Urresti, I.; Arrazola, P.J. (2009) Finite element modeling of oblique machining using an arbitrary Lagrangian–Eulerian formulation. *Machining Science and Technology: An International Journal*, 13(3): 385–406.

Lorentzon, J.; Järvstråt, N.; Josefson, B.L. (2009) Modelling of chip formation of alloy 718. *Journal of Materials Processing Technology*, 209: 4645–4653.

Madhavan, V.; Adibi-Sedeh, A.H. (2005) Understanding of finite element analysis results under the framework of Oxley's machining model. *Machining Science and Technology: An International Journal*, 9(3): 345–368.

Marusich, T.D.; Ortiz, M. (1995) Modeling and simulation of high-speed machining. *International Journal for Numerical Methods in Engineering*, 38: 3675–3694.

Merchant, M.E. (1945) Mechanics of the metal cutting process. *Journal of Applied Physics*, 16: 318–324.

Mitrofanov, A.V.; Babitsky, V.I.; Silberschmidt, V.V. (2003) Finite element simulations of ultrasonically assisted turning, *Computational Materials Science*, Volume 28, Issues 3–4, November 2003, pp. 645–653.

Mitrofanov, A.V.; Babitsky, V.I.; Silberschmidt, V.V. (2004) Finite element analysis of ultrasonically assisted turning of Inconel 718. *Journal of Materials Processing Technology*, 153–154: 233–239.

Mitrofanov, A.V.; Babitsky, V.I.; Silberschmidt, V.V. (2005) Thermomechanical finite element simulations of ultrasonically assisted turning. *Computational Materials Science*, 32(3–4): 463–471.

Molinari, A.; Moufky, A. (2005) A new thermomechanical model of cutting applied to turning operations. Part I. Theory. *International Journal of Machine Tools and Manufacture*, 45: 166–180.

Nasr, M.N.A.; Ng, E.-G.; Elbestawi, M.A. (2008) A modified time-efficient FE approach for predicting machining-induced residual stresses. *Finite Elements in Analysis and Design*, 44(4): 149–161.

Olschewski, J.; Hamann, A.; Bendig, M.; et al. (2001) Werkstoffmechanik einer Nickelbasislegierung beim Hochgeschwindigkeitsspanen-Werkstoffverhalten und Modellierung, Teil II, Report BAM-V.2 01/3. *Bundesanstalt für Materialforschung und prüfung* (BAM), Berlin.

Outeiro, J.C.; Pina, J.C.; M'Saoubi, R.; Pusavec, F.; Jawahir, I.S. (2008) Analysis of residual stresses induced by dry turning of difficult-to-machine materials. *CIRP Annals - Manufacturing Technology*, 57(1): 77–80.

Oxley, P.L.B. (1962) An analysis for orthogonal cutting with restricted tool-chip contact. *International Journal of Mechanical Sciences*, 4:129–125.

Özel, T. (2009a) Computational modelling of 3-D turning with variable edge design tooling: influence of micro-geometry on forces, stresses, friction and tool wear. *Journal of Materials Processing Technology*, 209(11): 5167–5177.

Özel, T. (2009b) Experimental and finite element investigations on the influence of tool edge radius in machining nickel-based alloy. *CD Proceedings of 2009 ASME International Conference on Manufacturing Science and Engineering*, Paper No. 84362, October 5–7 (2009). Lafayette, Indiana, USA.

Özel, T.; Zeren E. (2007) Finite element modeling of stresses induced by high speed machining with round edge cutting tools. *International Journal of Advanced Manufacturing Technology*, 35(3–4): 255–267.

Pantalé, O.; Rakotomalala, R.; Touratier, M. (1998) An A.L.E. three-dimensional model of orthogonal and oblique metal cutting processes. *International Journal of Forming Processes*, 1(3): 371–389.

Pawade, R.S.; Joshi, S.S.; Brahmankar, P.K. (2008) Effect of machining parameters and cutting edge geometry on surface integrity of high-speed turned Inconel 718. *International Journal of Machine Tools & Manufacture*, 48: 15–28.

Pereira, J.M.; Lerch, B.A. (2001) Effects of heat treatment on the ballistic impact properties of Inconel 718 for jet engine fan containment applications. *International Journal of Impact Engineering*, 25: 715–733.

Pusavec, F.; Deshpande, A.; M'Saoubi, R.; Kopac, J.; Dillon, O.W.; Jawahir, I.S. (2008) Predictive Performance Models and Optimization for Sustainable Machining of a High Temperature Nickel Alloy, Proceedings of High Performance Cutting, Dublin, pp. 335_345.

Rahman, M.; Seah, W.K.H.; Teo, T.T. (1997) The machinability of Inconel 718. *Journal of Materials Processing Technology*, 63: 199–204.

Ranganath, S.; Guo, C.; Hegde, P.A. (2009) Finite element modeling approach to predicting white layer formation in nickel superalloys. *CIRP Annals – Manufacturing Technology* 58: 77–80.

Sekhon, G.S.; Chenot, J.L. (1992) Some simulation experiments in orthogonal cutting. *Numerical Methods in Industrial Forming Processes*, Rotterdam, The Netherlands: A.A. Balkema, pp. 901–906.

Sharman, A.R.C.; Hughes, J.J.; Ridgway, K. (2004) Workpiece surface integrity and tool life issues when turning Inconel 718 nickel based superalloy. *Machining Science and Technology*, 8(3): 399–414.

Sievert, R.; Noack, H.D.; Hamann, A.; Loewe, P.; Singh, K.N.; Kuenecke, G.; Clos, R.; Schreppel, U.; Veit, P.; Uhlmann, E.; Zettier, R. (2003) Simulation der Spansegmentierung beim Hochgeschwindigkeits-Zerspanned unter Berücksichtigung duktiler Schädigung. *Techniche Mechanik*, Band 23, Heft 2–4, pp. 216–233.

Soo, S.L.; Aspinwall, D.K.; Dewes, R.C. (2004) Three-Dimensional Finite Element Modelling of High-Speed Milling of Inconel 718. *Proceedings of the Institution of Mechanical Engineers, Part B: Journal of Engineering Manufacture*, 218: 1555–1561.

Tancret, F.; Sourmail, T.; Yescas, M.A.; Evans, R.W.; McAleese, C.; Singh, L.; Smeeton, T.; Bhadeshia, H.K.D.H. (2003) Design of a creep resistant nickel base superalloy for power plant applications Part 3–Experimental results. *Materials Science and Technology*, 19: 296–303.

Tay, A.O.; Stevenson, M.G.; Davis, G.D.V.; Oxley, P.L.B. (1976) A numerical method for calculating temperature distributions in machining from force and shear angle measurements. *International Journal of Machine Tool Design and Research*, 16: 335–349.

Trigger, K.J.; Chao, B.T. (1951) An analytical evaluation of metal cutting temperatures. *Transactions of ASME*, 73: 57–68.

Uhlmann, E.; Graf von der Schulenburg, M.; Zettier, R. (2007) Finite element modeling and cutting simulation of Inconel 718. *Annals of the CIRP*, 56(1): 61–64.

Warnecke, G.; Oh, J.D. (2002) A new thermo-viscoplastic material model for finite-element-analysis of the chip formation process. *Annals of the CIRP*, 51(1): 79–82.

Zhang, B.; Mynors, D.J.; Mugarra, A.; Ostolaza, K. (2004) Representing the superplasticity of Inconel 718. *Journal of Materials Processing Technology*, 153–154: 694–698.

Zhang, J.M.; Gao, Z.Y.; Zhuang, J.Y.; Zhong, Z.Y.; Janschek, P. (1997) Strain-rate hardening behavior of superalloy IN718. *Journal of Materials Processing Technology*, 70: 252–257.

Zorev, N.N. (1966) *Metal Cutting Mechanics*, Oxford: Pergamon Press.